Numerical study of the exchange-bias effect in nanoparticles with ferromagnetic core/ferrimagnetic disordered shell morphology

M. Vasilakaki and K. N. Trohidou
NCSR "DEMOKRITOS," Institute of Materials Science, 153 10 Athens, Greece
(Received 11 November 2008; revised manuscript received 22 January 2009; published 2 April 2009)

We have used the Monte Carlo simulation technique to investigate the effect of a ferrimagnetic disordered shell on the hysteresis behavior of composite magnetic nanoparticles with ferromagnetic core/ferrimagnetic disordered shell morphology. We have examined the cooling field (H_{cool}) dependence of the exchange bias (H_{ex}), the coercive field (H_c), and the remanent magnetization (M_r) and we find that an increase in H_{cool} results initially in an increase in H_{ex}, H_c, and M_r, while further increase in H_{cool} causes a reduction in H_{ex} and H_c, but M_r remains constant. Our simulations show that an increase in the shell thickness for a given core size enhances the exchange bias field and reduces the remanent magnetization, the vertical shift, and the training effect. We also find that a reduction in the core size for a given particle size results in an increase in both exchange bias and coercive field. This behavior is reversed as the temperature increases. Our results are in good agreement with experimental findings.

DOI: 10.1103/PhysRevB.79.144402 PACS number(s): 75.50.Tt, 75.40.Mg, 75.50.Bb, 75.50.Vv

I. INTRODUCTION

The exchange bias effect is observed in magnetic materials[1] with two different spin structures in contact and it is defined as the asymmetry, on the magnetic field axis, of their hysteresis loops. This asymmetry is caused by a unidirectional anisotropy, the exchange anisotropy, which is induced by the exchange coupling in the interface between the different spin structures, when they are cooled down in a static magnetic field (H_{cool}). The effect was first observed in Co/CoO composite nanoparticles[2] with ferromagnetic (FM) core and antiferromagnetic (AFM) shell morphology.

The discovery of the exchange anisotropy was followed by extensive studies of its effect on layered systems with a FM/AFM interface.[3] Subsequently it has also been reported in several types of composite nanoparticle systems,[4–6] including the ones with a ferromagnetic core and a ferrimagnetic (FI) disordered shell[7–10] and inverted structure composite nanoparticles.[11]

Many experiments had been concentrated on the effect of the surface oxidation on the magnetic properties of Fe nanoparticles. The surface and interface effects between the oxide shell and magnetically hard Fe core were considered responsible for the high coercivity values observed at low temperatures[5,8,12,13] and its drastic temperature dependence. The highest coercivity obtained in Ref. 13 at room temperature was 1050 Oe for a particle with a 14 nm core diameter and its value at 10 K was 1425 Oe, whereas in a sample with core diameter of 2.5 nm the coercivity decreased from a value of 3400 Oe at 10 K to a negligible value at 150 K. Thus, in smaller particles the temperature dependence of the coercivity is much stronger than in bigger particles. In smaller particles the Fe core feels much more the effect of the Fe oxide shell due to higher Fe oxide to Fe ratio. The strong decrease in coercivity with temperature has been attributed to the superparamagnetic behavior of the Fe oxide shell and its low blocking temperature. It is estimated that the Fe oxide shell becomes superparamagnetic at $T \sim 10-50$ K.[5,8]

In addition to the exchange bias shift a vertical shift (DM) of the hysteresis loops has been observed in FM/AFM core/shell nanoparticles[14] attributed to the uncompensated spins of the shell.[15] Also some systems with FM/AFM interface exhibit the training effect, namely, the change in the exchange bias field and the coercive field by repeating the hysteresis loops after the field cooling procedure.[1]

The exchange bias field (H_{ex}) and the coercive field (H_c) are expected to depend on the field cooling process and the strength of the applied field. There are many studies[16–20] mainly on FM/AFM bilayers which show that H_{ex} and H_c can be tuned by the strength of the cooling field. For low cooling field values the exchange bias and the coercive field increase although for higher cooling fields the magnetic behavior depends on the kind of the interfacial couplings. Fiorani *et al.*[21] in their study of granular systems where Fe particles are embedded in a Fe oxide matrix with a spin-glasslike phase[22,23] showed that H_{ex} and H_c depend on the cooling field and the temperature from which the cooling field process initiates. They attributed this behavior to the fact that depending on the cooling field value, an energetically favorable spin configuration at the spin-glass-like shell is selected through the exchange interaction between the frozen ferrimagnetic spins and the ferromagnetic spins at the interface.

We have previously investigated the exchange bias mechanism and the factors that influence the exchange bias behavior in FM core/AFM (Refs. 24–26) shell nanoparticles and the aging and the training effect of FM/FI (Refs. 27 and 28) nanoparticles with spin-glasslike shell nanoparticles.

Motivated by our previous works we have continued our study on isolated composite nanoparticles with a ferromagnetic core and ferrimagnetic disordered shell, in order to investigate the underlying mechanism of (a) the field cooling dependence of the exchange bias field H_{ex}, the coercive field H_c, and the remanent magnetization M_r; (b) the shell thickness dependence of H_{ex}, H_c, M_r and DM; (c) the influence of the core size on the H_{ex} and H_c; and (d) the temperature dependence of H_c and H_{ex}. Results are also presented for the

training effect. In all cases we discuss the differences in the magnetic behavior between the FM/FI and FM/AFM composite nanoparticles and thin films.

The paper is organized as follows. In Sec. II, we describe the model of the magnetic structure of the nanoparticles and the method of calculation of the exchange bias field, the coercive field, the remanent magnetization, and the vertical shift. In Sec. III we present numerical results of the dependence of these quantities on the cooling field strength, the core size, the shell thickness, the temperature and of the training effect of H_c and H_{ex}. A discussion of our results is given in Sec. IV.

II. MODEL

The simulated composite nanoparticles consist of a FM core and a FI disordered shell. They are spherical nanoparticles of a radius R expressed in lattice spacings on a simple cubic (sc) lattice. We have divided the nanoparticles into layers of thickness one lattice spacing each (see Fig. 1) in order to get a better understanding of the contribution to their magnetic behavior from each part separately. The outer shell layer of one lattice spacing thickness is the surface. The interface, of thickness two lattice spacings, consists of the last layer of the FM core and the first layer of the FI shell.

We use atomic-scale modeling where the spins interact with nearest-neighbor Heisenberg interactions and at each crystal site they experience a uniaxial anisotropy. The energy of the system includes the exchange interaction between the spins in the core, the shell and at the interface, the single-site anisotropy energy terms of the core, the shell, the FM and the FI interfaces, and the Zeeman energy term;

$$\begin{aligned}\mathcal{H} = & -J_{\text{core}} \sum_{i,j \in \text{core}} \vec{S}_i \cdot \vec{S}_j - J_{\text{shell}} \sum_{i,j \in \text{shell}} \vec{S}_i \cdot \vec{S}_j \\ & - J_{\text{IF}} \sum_{i \in \text{core}, j \in \text{shell}} \vec{S}_i \cdot \vec{S}_j - K_{\text{core}} \sum_{i \in \text{core}} (\vec{S}_i \cdot \hat{e}_i)^2 \\ & - K_{\text{shell}} \sum_{i \in \text{shell}} (\vec{S}_i \cdot \hat{e}_i)^2 - K_{\text{IF/FM}} \sum_{i \in \text{IF/FM}} (\vec{S}_i \cdot \hat{e}_i)^2 \\ & - K_{\text{IF/FI}} \sum_{i \in \text{IF/FI}} (\vec{S}_i \cdot \hat{e}_i)^2 - \vec{H} \cdot \sum_I \vec{S}_i. \end{aligned} \quad (1)$$

Here $\vec{S}_i$ is the atomic spin at site i and $\hat{e}_i$ is the unit vector in the direction of the easy axis at site i. We consider the magnitude of the atomic spins in the FI sublattices to be equal to 1 and 1.5, respectively. The core and the interface anisotropy are uniaxial along the z axis and the shell and surface anisotropy is randomly oriented. The exchange coupling constant of the core $J_{\text{core}}=J_{\text{FM}}$ is taken equal to 1 and of the shell $J_{\text{shell}}=-J_{\text{FM}}/2$ due to the fact that Curie temperature of the FM in the core is higher than the critical temperature of the FI in the shell. We set the interface coupling constant $J_{\text{IF}}=J_{\text{FM}}/2$,[25] so the interfacial interaction is taken as ferromagnetic.

The value of the loop shift on the field axis is expressed by the exchange field $H_{ex}=-(H_{\text{right}}+H_{\text{left}})/2$ and the coercivity is defined as $H_c=(H_{\text{right}}-H_{\text{left}})/2$ with H_{right} and H_{left} being the points where the loop intersects the field axis.

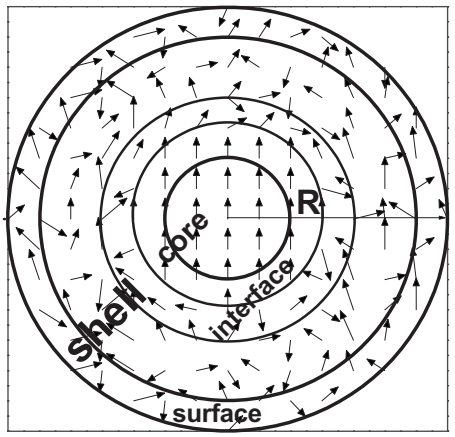

FIG. 1. A schematic representation of the simulated FM core/FI shell nanoparticle system.

The vertical shift (DM) is given by the expression DM $=(M_{\text{up}}+M_{\text{down}})/2$ with M_{up} and M_{down} being the values of the points where the loop intersects the magnetization axis. M_r is normalized to the magnetization at saturation M_s.

The fields H, H_c, and H_{ex} are given in units of $J_{\text{FM}}/g\mu_B$, the temperature T in units J_{FM}/k_B and the anisotropy coupling constants K in units of J_{FM}. The anisotropy constant for the core is $K_{\text{core}}=0.05J_{\text{FM}}$, for the ferromagnetic interface $K_{\text{IF/FM}}=0.5J_{\text{FM}}$ which is one order of magnitude larger than K_{core}, for the ferrimagnetic interface, the shell, and the surface $K_{\text{IF/FI}}=1.5J_{\text{FM}}$, $K_{\text{shell}}=1.5J_{\text{FM}}$, and $K_{\text{srf}}=1.5J_{\text{FM}}$, respectively. Although the surface anisotropy is considered to be the same with the shell anisotropy, we have distinguished the shell from the surface region because we want to study the contribution from each part separately. We introduce the strong random anisotropy in the shell and at surface in order to simulate a spin-glasslike phase.

We perform our calculations using the Monte Carlo (MC) simulation technique,[29] where the microstructure and the temperature are explicitly included. During the numerical procedure the hysteresis loops are calculated after the field cooling procedure under a static magnetic field. The magnetic field is always applied along the z axis. We simulate the field cooling procedure applying the H_{cool} starting at temperature $T=3.0J_{\text{FM}}/k_B$ above the critical temperature of the ferrimagnet (for the sc lattice $T_C=2.1J_{\text{FM}}/k_B$)[30] down to $T_f=0.01J_{\text{FM}}/k_B$ at a constant rate and then the hysteresis loop is measured.

For the MC simulations we have used the METROPOLIS algorithm. At this point it is useful to note that the time evolution of the system does not come from any deterministic equation for the magnetization; the dynamics obtained is intrinsic to the MC method.[29] This means that our time unit is not related to a real time interval. However, we stress the fact that we focus our attention on the role of the interface interactions and the random shell anisotropy on the magnetization and magnetization reversal processes and not on the determination of values for the relaxation times. The results were averaged over 40 different samples (namely, independent random number sequences) cooled down under the same conditions.

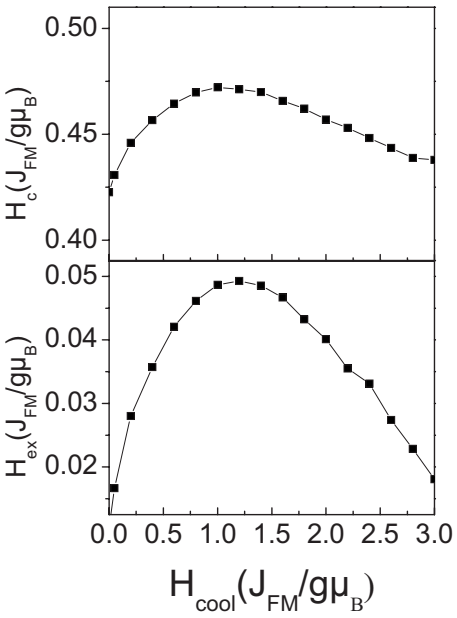

FIG. 2. Cooling field dependence of the coercive field (H_c) and the exchange bias field (H_{ex}) for a nanoparticle with core size five lattice spacings and shell thickness of seven lattice spacings.

III. RESULTS AND DISCUSSION

We present in this section results on spherical magnetic nanoparticles with FM core/FI disordered shell morphology. The parameters used in the model are the total nanoparticle size R, the core size and the shell thickness of the nanoparticles, the exchange coupling J in the core, in the shell and at the interface, and the anisotropy coupling constants K for the core, the interface, the shell, and the surface of the nanoparticle. Results are presented for several particle sizes using the values of J's and K's described in Sec. II, in order to discuss the physics emerging from some morphology characteristics of these systems.

We first examine the cooling field dependence of the H_{ex}, H_c, and M_r. Figure 2 shows the exchange bias and the coercive field as a function of the applied cooling field for a nanoparticle with FM core five lattice spacings and FI shell seven lattice spacings. Initially as the H_{cool} increases it causes an increase in both H_{ex} and H_c. The gradual increase in H_{cool} tends to align a certain amount of FI spins at the interface along the field direction. After some H_{cool} value further increase in the cooling field results in a decrease in these two quantities. In this case, for these higher cooling field values the Zeeman coupling between the field and the FI spins dominates the magnetic interactions inside the system. So the FI spins follow the applied field and as a result the exchange bias field and the coercive field decrease. Studies on the cooling field dependence of the H_{ex} that have been reported for systems of FM/AFM ultrafine particles[31] have shown that the H_{ex} increases with the increasing cooling field and then saturates for field values above 20 kOe. This cooling field behavior is attributed to the polarization of uncompensated spins as the cooling field is increased. In the case of FeF_2/Fe bilayers,[32] there is a decrease in H_{ex} for large enough cooling fields whereas for NiFe/CoO bilayers[19] the

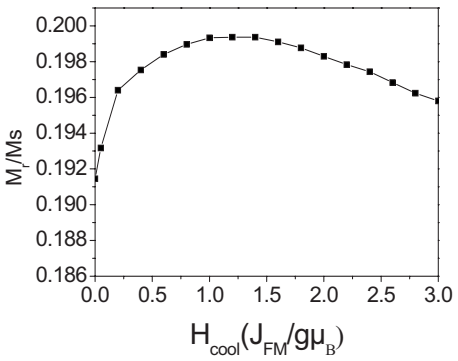

FIG. 3. Cooling field dependence of the remanent magnetization (M_r) normalized to the saturation magnetization (M_s) for a nanoparticle with core size of five lattice spacings and shell thickness of seven lattice spacings.

H_{ex} increases and for large enough cooling fields saturates. This behavior is attributed to the weaker anisotropy of FeF_2 as compared to CoO. Whereas in our case the existence of the spin-glasslike phase gives the downturn of the H_{ex} for large cooling fields. This is also the case for other FM/AFM based systems involving spin disorder.[18]

Figure 3 displays the cooling field dependence of the remanent magnetization for the same nanoparticle. For low cooling field values, M_r increases due to the increase in the alignment of the FI spins and then tends to saturate because most of the spins have been aligned along the cooling field direction. Our MC results reproduce very well the behavior of the cooling field dependence of H_c, H_{ex}, and M_r of Fe/FeO nanoparticles systems in Refs. 33 and 34.

We also study the effect of the shell thickness on the cooling field dependence of the coercive and the exchange bias field. In Fig. 4 we present our results for the cooling field dependence of H_c and H_{ex} for a nanoparticle with core radius of five lattice spacings and shell thickness of nine lattice spacings. From Fig. 4 we see that the variation of H_c and H_{ex} with the cooling field have similar behavior to that observed in Fig. 2, but the increase in the FI disordered shell thickness results in an increase in the size for both H_{ex} and H_c. The increase is more pronounced in H_c because we have bigger contribution from the disordered shell, and less in H_{ex}, confirming the fact that the major contribution of H_{ex} comes from the interface while in the H_c we have contribution from the whole particle.

Next, we study the influence of the shell thickness in the behavior of the hysteresis loop and on the thermal dependence of the coercive and the exchange bias field, starting the field cooling procedure with a field $H_{cool}=0.4J/g\mu_B$ at $T=3.0J_{FM}/k_B$. We consider four particles with total radii $R=9.0$, $R=12.0$, $R=14.0$, and $R=20.0$ lattice spacings. They all have the same core size of five lattice spacings and FI shell thicknesses of 4, 7, 9, and 15 lattice spacings, respectively. The surface thickness is one lattice spacing in all cases. The results for the hysteresis loops for these four particles are shown in Fig. 5 at a very low temperature $T=0.01J_{FM}/k_B$. As we can see the hysteresis loops are shifted and the nanoparticles with the bigger shell thickness have the bigger shift and the bigger coercive field. So both

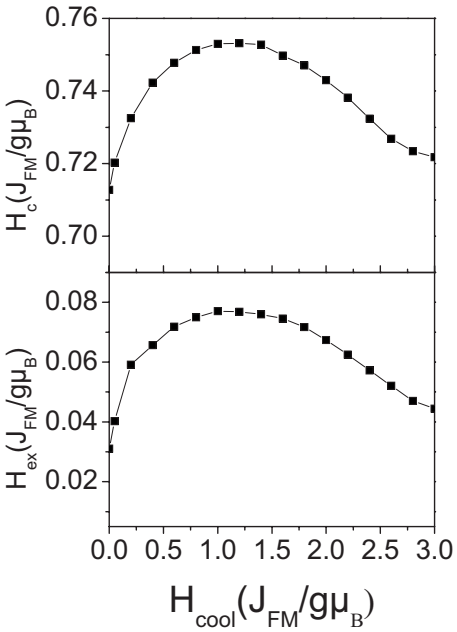

FIG. 4. Cooling field dependence of H_c and H_{ex} for a nanoparticle with core size of five lattice spacings and shell thickness of nine lattice spacings.

H_c and H_{ex} increase with the shell thickness while M_r decreases. This is in agreement with the experimental findings of Baker and his collaborators[34] on Fe/FeO nanoparticles. We also observe a small vertical shift in the hysteresis loops of the two nanoparticles with the smaller shell thickness. The asymmetry in the magnetization axis disappears for the two bigger nanoparticles. The hysteresis loop for the nanoparticle with the lower shell thickness has a shoulder, which is characteristic of a two-phase system.[35–37] This shoulder disappears as the shell thickness increases because the shell dominates in the hysteresis behavior of the sample. In Fig. 5 we observe that the hysteresis loops of the nanoparticles with the bigger shell thickness are less saturated due to the enhancement of the spin-glass-like behavior.[23,38]

To further demonstrate the role of the shell, we keep the core size constant and we increase the shell thickness. Our results are presented in Fig. 6 where we have plotted H_c, H_{ex}, M_r, and the vertical shift DM as functions of the shell thickness. In this case we have started with a ferromagnetic nanoparticle with core radius of five lattice spacings and we add ferrimagnetic layers. From Fig. 6 we observe that: (a) the coercive field increases continuously with the shell thickness, (b) H_{ex} increases slowly with the increase in the shell thickness and then it remains constant, (c) the remanent magnetization has an exponential decay with the shell thickness, and (d) the vertical shift also decreases with the shell size and vanishes after a critical size. The increase in H_c with the increase in the disordered layer is expected due to the fact that the thicker shell has bigger number of disordered spins. Our MC results agree with the experimental findings for Fe/Fe oxide core/shell nanoparticles by Baker *et al.*[34] In experimental studies of FM/AFM (Refs. 3, 39, and 40) or FI bilayers[5] and Co/CoO (Ref. 6) nanoparticles, they found that H_{ex} increases and then saturates for large AFM thickness. In

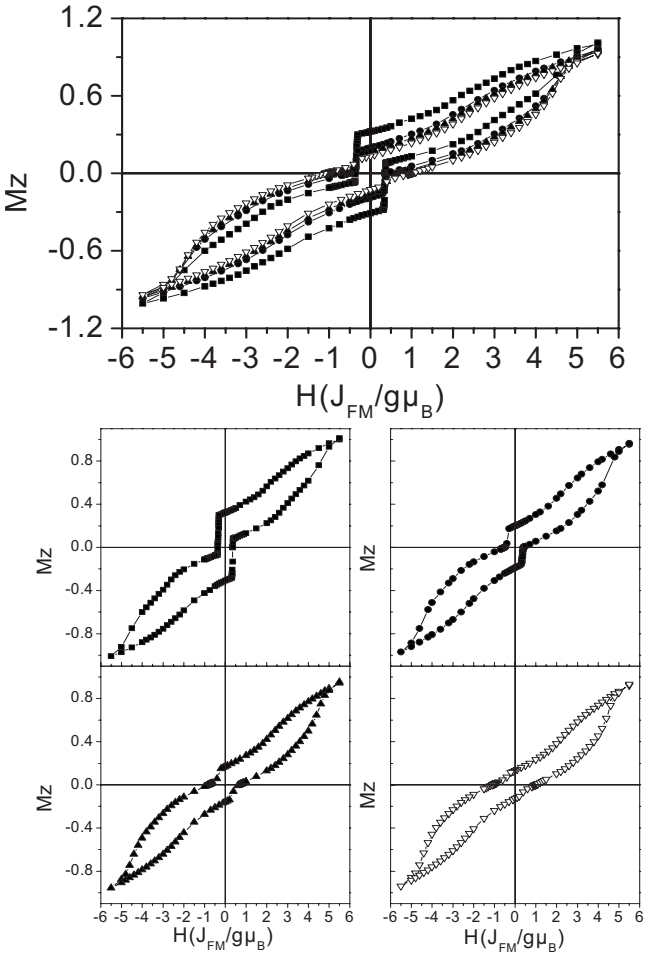

FIG. 5. Hysteresis loops of core/shell nanoparticles with core radius R_c=5 lattice spacings and shell thicknesses of 4 (■), 7 (●), 9 (▲), and 15 (▽) lattice spacings, respectively.

our previous study[26] on nanoparticles with AFM shell we found that at low temperature the H_{ex} increases rapidly with the shell thickness and then remains constant up to a shell thickness comparable to the size of the core, while for further increase in the shell thickness it decreases. We have attributed this behavior to the increase in the AFM character in the

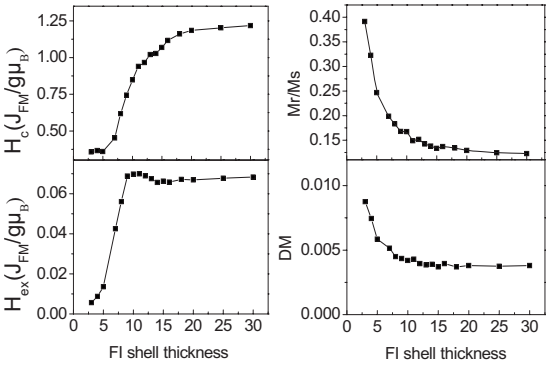

FIG. 6. Shell thickness dependence of the coercive field (H_c), the exchange bias field (H_{ex}), the normalized remanent magnetization (M_r/M_s), and the vertical shift (DM) with core radius R_c=5 lattice spacings.

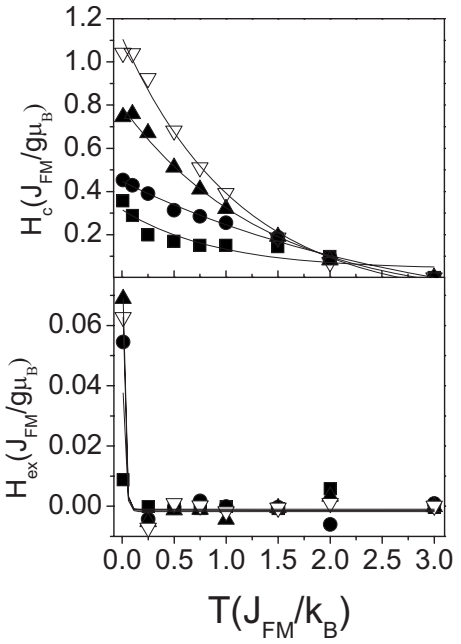

FIG. 7. Temperature dependence of H_c and H_{ex} for nanoparticles with core radius $R_c=5$ lattice spacings and shell thicknesses of 4 (■),7 (●), 9 (▲), and 15 (▽) lattice spacings, respectively.

nanoparticle. We expect that in the case of the FI disordered shell the reduction will also occur but for much bigger shell thickness than in the AFM ordered shell case. The remanent magnetization is reduced because the disorder is enhanced with the increase in the ferrimagnetic shell, so its magnetic contribution is diminished as it has also been observed experimentally.[34,41] The behavior of the vertical shift confirms the fact that DM originates from the uncompensated spins in the shell as in the AFM shell case.[15] Thus as the shell thickness increases, the number of the uncompensated spins[26] relatively to the total number of the spins in the nanoparticle decreases; subsequently DM decreases. We must noticed here that there are situations where the observed loop shifts are coming from minor loops.[11] However our simulations for the hysteresis loops are extended to applying field values that assure that we are not in the minor loops field range.

Also we have studied the temperature dependence of H_c and H_{ex} for FI shell thicknesses of 4, 7, 9, and 15 lattice spacings. In Fig. 7 we show the coercive field and the exchange bias field, respectively, as functions of temperature. We observe that H_{ex} decreases rapidly with increasing temperature, because the interface interaction is masked by the thermal fluctuations. We also observe that the decrease in H_{ex} is exponential as it is observed experimentally in Ref. 34. Baker *et al.*[34] showed a fast decay of H_{ex} with temperature similar to that in Fig. 7. The coercive field also exhibits an exponential decay with temperature for bigger shell thickness in agreement with the experimental findings in Ref. 42. The observed temperature dependence of H_c and H_{ex} is different from that reported in FM/AFM bilayers[20,43] and FM/AFM nanoparticles.[2,24,25,44]

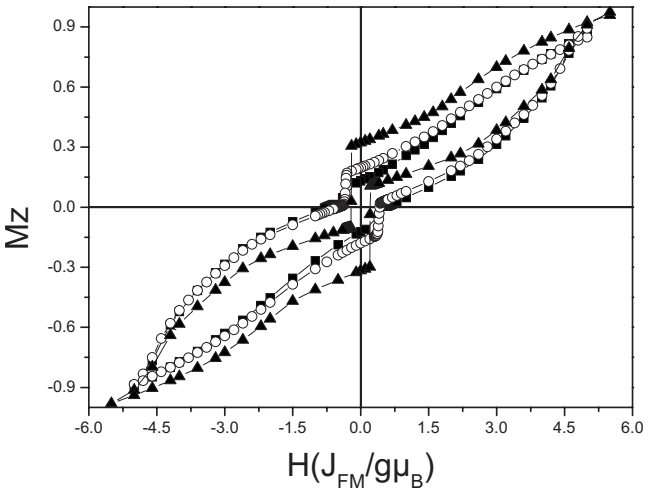

FIG. 8. Hysteresis loops of nanoparticles with shell thickness of seven lattice spacings and core sizes of three (■), five (○), and ten (▲) lattice spacings, respectively.

Next we consider the core size dependence of the exchange bias field and the coercive field. In Fig. 8 we present results for the hysteresis loops for three nanoparticles with the same shell thickness of seven lattice spacings and three different core sizes of three, five, and ten lattice spacings at a very low temperature $T=0.01J_{FM}/k_B$. As we can see, the hysteresis loops are shifted and the nanoparticle with the smaller core radius have the bigger coercive and exchange bias field, in agreement with the experimental findings of references.[8,45–47] This is due to the fact that the biggest contribution from the interface is obtained in the nanoparticle with the smallest core radius.

In Fig. 9 the coercive and exchange bias fields are displayed as functions of temperature for these nanoparticles of constant shell thickness. It can be seen that at low temperatures there is a size reversal to the temperature dependence of the coercive and exchange bias fields. The coercive field is decreasing faster with temperature in the case of the smaller core nanoparticles than in the bigger ones. There is a crossing temperature above which the behavior is changed and the nanoparticles with the bigger core radius have higher coercivity. This is the temperature at which the shell becomes totally disordered. Above this temperature the coercivity follows the temperature dependence of the core. The smaller in size core becomes faster superparamagnetic. This is in agreement with experimental findings by Gangopadhyay *et al.*[47] on Fe nanoparticles surrounded by a disordered iron oxide shell. In the case of the two smaller nanoparticles the H_c decays exponentially as in the case of the varying shell thickness (see Fig. 7) due to the dominance of the disordered shell. For the biggest nanoparticle H_c has a monotonic temperature dependence due to the dominant ferromagnetic character. The exchange bias field vanishes very quickly with the increase in the temperature.

Finally we study the training effect on H_c and H_{ex} for the nanoparticles. This effect is present in the FM core/FI spin-glasslike shell systems since one of the characteristics of spin-glass systems is their multiple configuration of the ground state.[23] So the frozen spins, which are originally

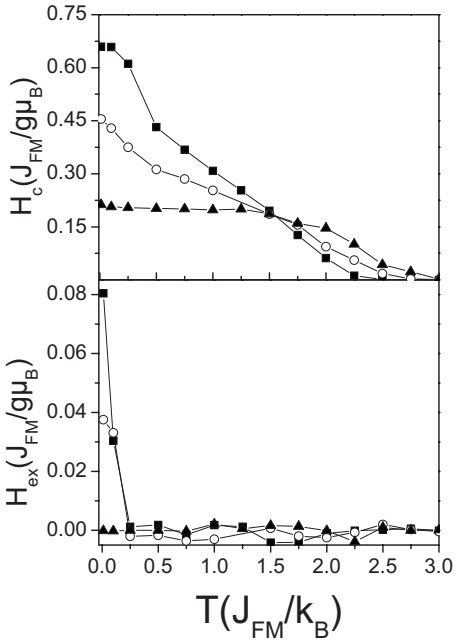

FIG. 9. H_c and H_{ex} as a function of temperature for nanoparticles with shell thickness of seven lattice spacings and core sizes of three (■), five (○), and ten (▲) lattice spacings, respectively.

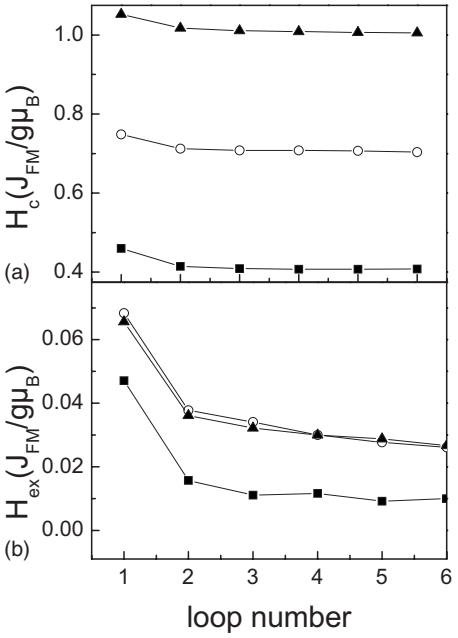

FIG. 10. Training effect of (a) H_c and (b) H_{ex} for core/shell nanoparticles with core size of five lattice spacings and shell thicknesses of 7 (■), 9 (○), and 15 (▲) lattice spacings, respectively.

aligned in the cooling field direction, may change their directions and fall into other metastable configurations during the hysteresis measurements. This characteristic of spin-glasslike phase essentially influences the exchange bias behavior of the system and results in a decrease in H_c and H_{ex} with the field cycling. The behavior of the training effect for the composite FM core/FI spin-glasslike shell nanoparticles will depend on its microstructure characteristics. Indeed in Fig. 10 we have plotted H_{ex} and H_c as functions of the loop cycling for three nanoparticles with core radius of five lattice spacings and shell thicknesses of 7, 9, and 15 lattice spacings. Following the same field cooling process as above, with cooling field $H_{cool}=0.4J_{FM}/g\mu_B$, the hysteresis loop was calculated six consecutive times at temperature $T=0.01J_{FM}/k_B$. We observe that H_{ex} in the case of the nanoparticle with shell thickness of seven lattice spacings after the first loop has a big reduction, while H_{ex} for the other two nanoparticles has a small reduction with the loop cycling and very similar. These two nanoparticles have the same size of the exchange bias field as it can be seen from Fig. 6. H_c has a bigger reduction with the loop cycling for the smaller shell nanoparticle than in the other two. This behavior indicates that the interface has the major contribution in the training effect for the chosen nanoparticles. As the shell thickness decreases we expect contribution from the shell and the core to the training effect. So a ~50% reduction in H_{ex} during cycling has been observed in FM/FI nanoparticles,[9,27] with small shell thickness, whereas a ~12% reduction in the case of Co/CoO nanoparticles.[6] In any case we expect that the behavior of the training effect depends not only on the magnetic microstructure but also on other factors, in agreement with the experimental observations in FM/AFM bilayer systems.[1]

IV. CONCLUSION

We have presented a systematic study on the coercive behavior of composite nanoparticles consisting of a ferromagnetic core and a ferrimagnetic disordered shell. We assumed Heisenberg exchange interaction between the spins in the nanoparticle. Our simulations show that: (a) the cooling field value affects the hysteresis behavior of the nanoparticles with spin-glasslike shell in agreement with the experimental findings, (b) the increase in the shell thickness results in an increase in the coercivity and the exchange bias field and a decrease in the remanent magnetization as it has been observed experimentally, (c) at low temperatures there is a reversal in the core size dependence of coercivity and the exchange bias field, namely, the smaller nanoparticles have the higher values of H_{ex} and H_c, and (d) the behavior of the training effect depends on the shell thickness for a given magnetic microstructure. The exchange bias field in all cases disappears at temperature where the shell becomes totally disordered, while above this temperature the coercive field is higher for the bigger nanoparticle.

In the present study we consider isolated nanoparticles in order to investigate the exchange bias mechanism and the dependence of the exchange bias effects on the nanoparticle's microstructure. We expect that the interparticle interactions will affect the coercive behavior of the nanoparticles. However our preliminary results[48] on FM/AFM nanoparticles and recent experimental findings[49,50] indicate that in order to determine the behavior of composite nanoparticle assemblies one has to take into account the microstructure of the nanoparticle and their description certainly has to go beyond the Stoner-Wohlfarth single-spin model.[51]

ACKNOWLEDGMENTS

The authors would like to thank D. Fiorani and G. Hadgipanayis for useful discussions. The work was supported by EU STREP Project No. NMPCT-2004-013545 Nanospin (Self-Organized Complex-Spin Magnetic Nano-Structures). Finally, we would like to acknowledge the memory of A. Kostikas who stimulated our work at its very beginning.

[1] J. Nogues, J. Sort, V. Langlais, V. Skumryev, S. Surinach, J. S. Munoz, and M. D. Baro, Phys. Rep. **422**, 65 (2005).
[2] W. H. Meiklejohn and C. P. Bean, Phys. Rev. **105**, 904 (1957).
[3] J. Nogues and I. K. Schuller, J. Magn. Magn. Mater. **192**, 203 (1999).
[4] J. Nogues, J. Sort, V. Langlais, S. Doppiu, B. Dieny, J. S. Munoz, S. Surinach, M. D. Baro, S. Stoyanov, and Y. Zhang, Int. J. Nanotechnol. **2**, 23 (2005); R. H. Kodama, A. E. Berkowitz, E. J. McNiff, and S. Foner, Phys. Rev. Lett. **77**, 394 (1996); P. J. van der Zaag, R. M. Wolf, A. R. Ball, C. Bordel, L. F. Feiner, and R. Jungblut, J. Magn. Magn. Mater. **148**, 346 (1995).
[5] X. Lin, A. S. Murthy, G. C. Hadjipanayis, C. Swann, and S. I. Shah, J. Appl. Phys. **76**, 6543 (1994).
[6] D. L. Peng, K. Sumiyama, T. Hihara, S. Yamamuro, and T. J. Konno, Phys. Rev. B **61**, 3103 (2000).
[7] J. Sort, V. Langlais, S. Doppiu, B. Dieny, S. Surinach, J. S. Munoz, M. D. Baro, Ch. Laurent, and J. Nogues, Nanotechnology **15**, S211 (2004).
[8] L. Del Bianco, D. Fiorani, A. M. Testa, E. Bonetti, L. Savini, and S. Signoretti, J. Magn. Magn. Mater. **262**, 128 (2003); Phys. Rev. B **66**, 174418 (2002).
[9] D. L. Peng, T. Hihara, K. Sumiyama, and H. Morikawa, J. Appl. Phys. **92**, 3075 (2002).
[10] L. Del Bianco, A. Hernando, M. Multigner, C. Prados, J. C. Sanchez-Lopez, A. Fernadez, C. F. Conde, and A. Conde, J. Appl. Phys. **84**, 2189 (1998); S. Banerjee, S. Roy, J. W. Chen, and D. Chakravorty, J. Magn. Magn. Mater. **219**, 45 (2000); L. Del Bianco, D. Fiorani, A. M. Testa, and E. Bonetti, *ibid.* **290-291**, 102 (2005).
[11] G. Salazar-Alvarez, J. Sort, S. Surinach, M. Dolors Baro, and J. Nogues, J. Am. Chem. Soc. **129**, 9102 (2007).
[12] S. Yamamuro, K. Simiyama, T. Kamiyama, and K. Suzuki, J. Appl. Phys. **86**, 5726 (1999); C. M. Hsu, H. M. Lin, K. R. Tsai, and P. Y. Lee, *ibid.* **76**, 4793 (1994).
[13] S. Gangopadhyay, G. C. Handjipanayis, C. M. Sorensen, and K. J. Klabunde, in *Nanophase Materials*, edited by G. C. Hadjipanayis (Kluwer, Dordrecht, 1994), p. 573.
[14] E. C. Passamani, C. Larica, C. Marques, J. R. Provetti, A. Y. Takenchi, and F. H. Sanchez, J. Magn. Magn. Mater. **299**, 11 (2006).
[15] M. Vasilakaki, E. Eftaxias, and K. N. Trohidou, Phys. Status Solidi A **205**, 1865 (2008).
[16] T. Qian, G. Li, T. Zhang, T. F. Zhou, X. Q. Xiang, X. W. Kang, and X. G. Li, Appl. Phys. Lett. **90**, 012503 (2007).
[17] B. Kagerer, Ch. Binek, and W. Kleemann, J. Magn. Magn. Mater. **217**, 139 (2000); A. Paul, C. M. Schneider, and J. Stahn, Phys. Rev. B **76**, 184424 (2007); C. Luna, M. Morales, C. J. Serna, and M. Vazquez, Nanotechnology **15**, S293 (2004); D. Z. Yang, J. Du, L. Sun, X. S. Wu, X. X. Zhang, and S. M. Zhou, Phys. Rev. B **71**, 144417 (2005); J. Nogués, C. Leighton, and I. K. Schuller, *ibid.* **61**, 1315 (2000).
[18] Yan-kun Tang, Young Sun, and Zhao-hua Cheng, J. Appl. Phys. **100**, 023914 (2006); Phys. Rev. B **73**, 174419 (2006).
[19] T. Ambrose and C. L. Chien, J. Appl. Phys. **83**, 7222 (1998).
[20] C. Leighton, J. Nogues, B. J. Jonsson-Akerman, and I. K. Schuller, Phys. Rev. Lett. **84**, 3466 (2000).
[21] D. Fiorani, L. Del Bianco, and A. M. Testa, J. Magn. Magn. Mater. **300**, 179 (2006).
[22] M. Ali, P. Adie, C. H. Marrows, D. Greig, B. J. Hickey, and R. L. Stamps, Nature Mater. **6**, 70 (2007).
[23] K. Binder and A. P. Young, Rev. Mod. Phys. **58**, 801 (1986).
[24] X. Zianni and K. N. Trohidou, J. Phys.: Condens. Matter **10**, 7475 (1998).
[25] E. Eftaxias and K. N. Trohidou, Phys. Rev. B **71**, 134406 (2005), and references therein.
[26] E. Eftaxias, M. Vasilakaki, and K. N. Trohidou, Mod. Phys. Lett. B **21**, 1169 (2007).
[27] K. N. Trohidou, M. Vasilakaki, L. Del Bianco, D. Fiorani, and A. M. Testa, J. Magn. Magn. Mater. **316**, e82 (2007).
[28] D. Fiorani, L. Del Bianco, A. M. Testa, and K. N. Trohidou, J. Phys.: Condens. Matter **19**, 225007 (2007).
[29] K. Binder, in *Applications of Monte Carlo Methods in Statistical Physics*, edited by K. Binder (Springer, Berlin, 1984).
[30] S. Freeman and P. J. Wojtowicz, Phys. Rev. **177**, 882 (1969).
[31] S. M. Zhou, D. Imhoff, K. Yu-Zhang, and Y. Leprince-Wang, Appl. Phys. A: Mater. Sci. Process. **81**, 115 (2005).
[32] J. Nogues, D. Lederman, T. J. Moran, and I. K. Schuller, Phys. Rev. Lett. **76**, 4624 (1996).
[33] L. Del Bianco, D. Fiorani, A. M. Testa, E. Bonetti, and L. Signorini, Phys. Rev. B **70**, 052401 (2004).
[34] C. Baker, S. K. Hasanain, and S. Ismat Shah, J. Appl. Phys. **96**, 6657 (2004).
[35] X. H. Xu, T. Jin, H. S. Wu, F. Wang, X. L. Li, and F. X. Jiang, Thin Solid Films **515**, 5471 (2007).
[36] T. Li, H. Yan, H. Wang, and W. Zheng, Int. J. Mod. Phys. B **19**, 2261 (2005).
[37] Y. Xu, Z. G. Sun, Y. Qiang, and D. J. Sellmyer, J. Magn. Magn. Mater. **266**, 164 (2003).
[38] R. K. Zheng, G. H. Wen, K. K. Fung, and X. X. Zhang, J. Appl. Phys. **95**, 5244 (2004).
[39] M. S. Lund, W. A. A. Macedo, Kai Liu, J. Nogues, I. K. Schuller, and C. Leighton, Phys. Rev. B **66**, 054422 (2002).
[40] X. S. Liu, B. X. Gu, W. Zhong, H. Y. Jiang, and Y. W. Du, Appl. Phys. A: Mater. Sci. Process. **77**, 673 (2003).
[41] F. Jimenez-Villacorta and C. Prieto, J. Phys.: Condens. Matter **20**, 085216 (2008).
[42] E. Tronc, M. Noguès, C. Chanéac, F. Lucari, F. D'Orazio, J. M. Grenèche, J. P. Jolivet, D. Fiorani, and A. M. Testa, J. Magn. Magn. Mater. **272-276**, 1474 (2004).
[43] T. Ambrose, K. Leifer, K. J. Hemker, and C. L. Chien, J. Appl. Phys. **81**, 5007 (1997).
[44] S. Gangopadhyay, G. C. Hadjipanayis, C. M. Sorensen, and K. J.

Klabunde, Nanostruct. Mater. **1**, 449 (1992).
[45] K. N. Trohidou, C. M. Soukoulis, A. Kostikas, and G. Hadjipanayis, J. Magn. Magn. Mater. **104-107**, 1587 (1992).
[46] O. Bomati-Miguel, P. Tartaj, M. P. Morales, P. Bonville, U. Golla-Schindler, X. Q. Zhao, and S. Veintemillas-Verdaguer, Small **2**, 1476 (2006).
[47] S. Gangopadhyay, G. C. Hadjipanayis, B. Dale, C. M. Sorensen, K. J. Klabunde, V. Papaefthymiou, and A. Kostikas, Phys. Rev. B **45**, 9778 (1992).
[48] D. Kechrakos, K. N. Trohidou, and M. Vasilakaki, J. Magn. Magn. Mater. **316**, e291 (2007).
[49] J. Nogues, V. Skumryev, J. Sort, S. Stoyanov, and D. Givord, Phys. Rev. Lett. **97**, 157203 (2006).
[50] N. Domingo, A. T. Testa, D. Fiorani, C. Binns, S. Baker, and J. Tehada, J. Magn. Magn. Mater. **316**, 155 (2007).
[51] C. Binns, M. J. Maher, Q. A. Pankhurst, D. Kechrakos, and K. N. Trohidou, Phys. Rev. B **66**, 184413 (2002).